Cell, Vol. 112, 659–672, March 7, 2003, Copyright ©2003 by Cell Press

Tumor Suppressor NM23-H1 Is a Granzyme A-Activated DNase during CTL-Mediated Apoptosis, and the Nucleosome Assembly Protein SET Is Its Inhibitor

Zusen Fan,[1] Paul J. Beresford,[1] David Y. Oh, Dong Zhang, and Judy Lieberman*
Center for Blood Research and
Department of Pediatrics
Harvard Medical School
Boston, Massachusetts 02115

Summary

Granzyme A (GzmA) induces a caspase-independent cell death pathway characterized by single-stranded DNA nicks and other features of apoptosis. A GzmA-activated DNase (GAAD) is in an ER associated complex containing pp32 and the GzmA substrates SET, HMG-2, and Ape1. We show that GAAD is NM23-H1, a nucleoside diphosphate kinase implicated in suppression of tumor metastasis, and its specific inhibitor (IGAAD) is SET. NM23-H1 binds to SET and is released from inhibition by GzmA cleavage of SET. After GzmA loading or CTL attack, SET and NM23-H1 translocate to the nucleus and SET is degraded, allowing NM23-H1 to nick chromosomal DNA. GzmA-treated cells with silenced NM23-H1 expression are resistant to GzmA-mediated DNA damage and cytolysis, while cells overexpressing NM23-H1 are more sensitive.

Introduction

Cytotoxic T lymphocytes (CTL) induce apoptosis of virus-infected or tumor cells by releasing cytolytic granules containing a pore-forming protein, perforin, and granzyme (Gzm) serine proteases (reviewed in Russell and Ley 2002). Gzms are delivered into the target cell cytosol by perforin. GzmB triggers apoptosis via caspase-dependent and -independent mechanisms (Sarin et al., 1997), which involve direct cleavage of downstream caspase substrates. The tryptase GzmA, the most abundant Gzm in CTL and NK cells, induces an alternate caspase-independent pathway with features of apoptosis, although DNA is damaged by single-stranded nicks, not oligonucleosomal fragmentation (Beresford et al., 1999; Shresta et al., 1999). Target cells resistant to GzmB or the caspases, such as tumors overexpressing bcl-2, are susceptible to GzmA (Beresford et al., 1999).

Affinity chromatography with the inactive Ser-Ala mutant (S-AGzmA) was used to isolate potential GzmA substrates (Beresford et al., 1997). A 270–420 kDa ER-associated complex (SET complex) that binds to immobilized S-AGzmA contains the tumor suppressor pp32 and three GzmA substrates: the nucleosome assembly protein (NAP) SET, the DNA bending protein HMG2, and the base excision repair enzyme Ape1/Ref-1 (Beresford et al., 2001; Fan et al., 2002, 2003). Overexpression of pp32 (also known as PHAPI, I_1^{PP2A}), an inhibitor of protein phosphatase 2A, causes cell cycle arrest and suppresses oncogene transformation (Bai et al., 2001; Li et al., 1996). The NAP activity of SET (also known as PHAPII, TAF-Iβ, I_2^{PP2A}) is abrogated by GzmA degradation (Beresford et al., 2001). SET has been postulated to link the transcription complex and chromatin (Seo et al., 2001; Shikama et al., 2000). SET (with its homolog TAF-Iα) and pp32 (and its homolog APRIL) are in a ~150 kDa nuclear complex that inhibits histone acetylation and DNA demethylation and binds HuR, which stabilizes immediate early gene mRNAs (Brennan et al., 2000; Cervoni et al., 2002; Seo et al., 2001, 2002).

The 270–450 kDa SET complex, which contains SET, pp32, HMG-2, and Ape1, also contains an unidentified GzmA-activated DNase (GAAD). GzmA-mediated DNA nicking is reconstituted by incubating isolated nuclei with GzmA-treated SET complex, but not with untreated SET complex (Beresford et al., 2001). Here, we identify GAAD as the tumor metastasis suppressor NM23-H1 and show that its specific inhibitor (IGAAD) is SET. NM23-H1 belongs to a gene family with eight human members (Lacombe et al., 2000). NM23 genes play critical roles in cellular proliferation, embryonic development, differentiation, oncogenesis, and tumor metastasis (reviewed in Lascu 2000). The mechanisms for these pleiomorphic effects are not well understood. NM23 proteins are evolutionarily conserved NDP kinases originating in bacteria, where they catalyze the transfer of γ-phosphates between NTPs and NDPs. NM23-H1 and NM23-H2, the best-studied NM23 proteins, are highly homologous (88% amino acid identity) but have distinct functions; NM23-H1 was first identified as a tumor metastasis suppressor (Steeg et al., 1988), and NM23-H2 activates *c-myc* transcription. Both proteins bind and nick the nuclease-hypersensitive element of the *c-myc* promoter (Postel, 1999). NM23-H1 also recognizes the 5′-SHS silencer and the NHE basal promoter of *PDGF-A* as substrates for DNA nicking (Ma et al., 2002).

NM23-H1, but not NM23-H2, is in the SET complex and has DNase activity, which SET inhibits. GzmA cuts SET, removing the inhibition, and triggers NM23-H1 to move to the nucleus where it nicks chromosomal DNA. This work provides the description of a DNA damage mechanism in caspase-independent cell death.

Results

GzmA Induces DNA Single-Stranded Nicks

Loading target cells with GzmA and perforin fails to induce oligonucleosomal DNA fragmentation, measured by agarose gel electrophoresis, release of detergent soluble DNA fragments, or TdT labeling (Beresford et al., 1999; data not shown). However, single-stranded breaks, identified by radiolabeling nicked ends with Klenow and denaturing agarose gel electrophoresis, are detected within 4 hr (Figures 1A and 1B). DNA is not damaged by treatment with GzmA or perforin alone or with perforin and S-AGzmA. DNA breaks can also be visualized in situ by nick translation using Klenow-cata-

*Correspondence: lieberman@cbr.med.harvard.edu
[1]These authors contributed equally to this work.

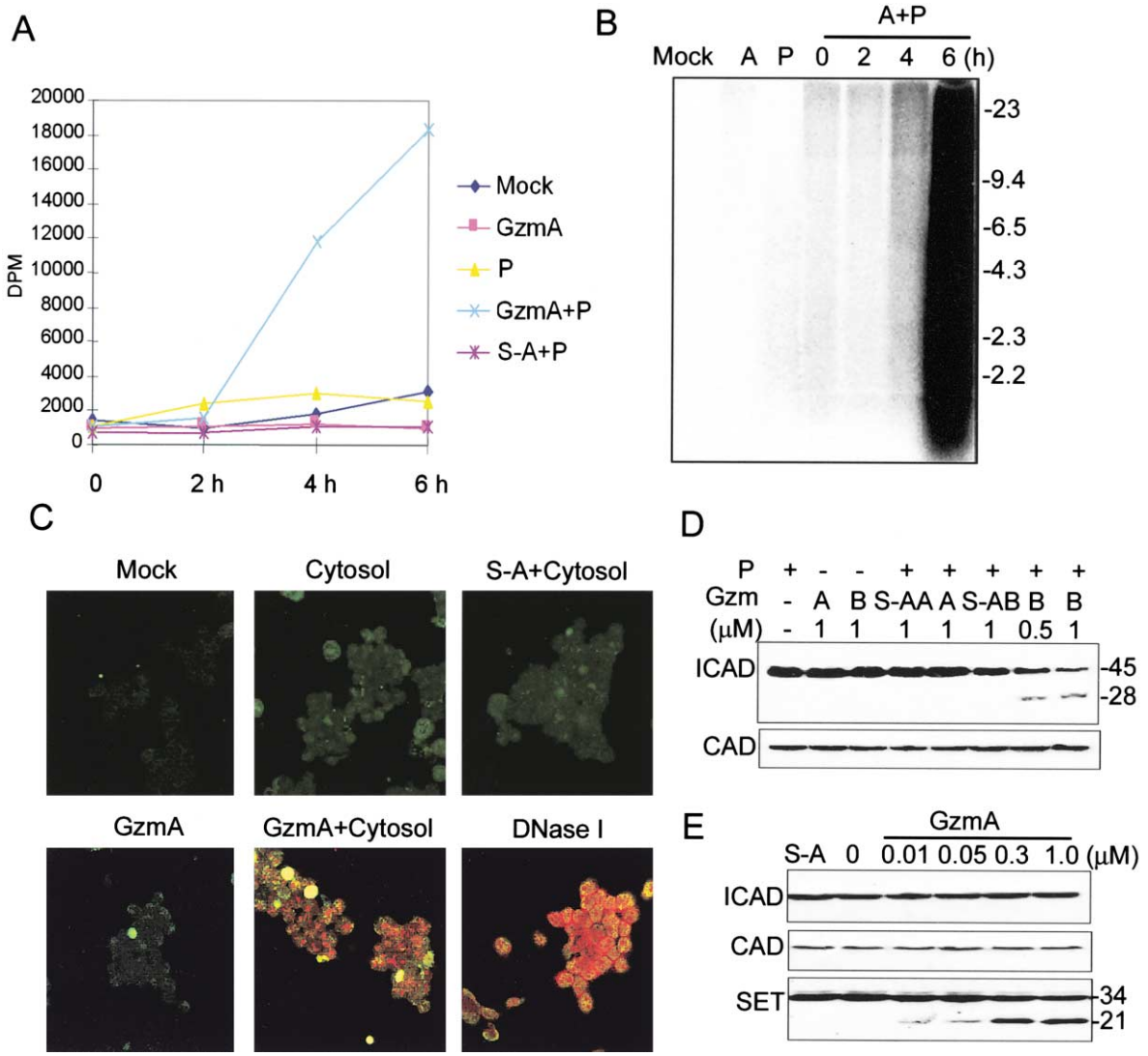

Figure 1. GzmA and Perforin Induce Single-Stranded DNA Nicks

(A and B) Loading GzmA, but not S-AGzmA, into K562 cells with perforin (P) induces DNA damage within 4 hr. Klenow-radiolabeled nicked DNA in isolated treated nuclei was analyzed by scintillation counting (A) and denaturing agarose gel electrophoresis (B).

(C) DNA nicks after GzmA treatment of isolated nuclei, observed by in situ fluorescence, requires active enzyme and cytosol. Isolated K562 nuclei were treated with GzmA or S-AGzmA with or without cytosol. Nicks were labeled with Alexa 568-dUTP (red), and SYTOX green was used for counterstaining. DNase I is a positive control.

(D) ICAD/DFF45, but not CAD, is degraded in cells perforin-loaded with GzmB (B), but not with GzmA (A) or the S-A mutants (S-AB, S-AA). Lysates were analyzed by immunoblot 4 hr after loading.

(E) ICAD is not cleaved when K562 cell lysates are incubated directly with GzmA for 2 hr at 37°C. S-AGzmA was at 1 μM. SET is probed as positive control.

lyzed incorporation of fluorophore-labeled dUTP (Figure 1C). Labeling isolated K562 nuclei by GzmA requires a small amount of cytosol plus active enzyme and occurs throughout the condensed chromatin and along the nuclear envelope (Figure 1C).

The caspase-activated DNase (DFF40/CAD) makes blunt double-stranded breaks after its inhibitor DFF45/ICAD is cleaved by caspases (Enari et al., 1998; Liu et al., 1997). GzmB cuts ICAD directly or indirectly by activating caspases (Sharif-Askari et al., 2001; Thomas et al., 2000), but GzmA loading with perforin (Figure 1D) or treatment of cell lysates (Figure 1E) does not lead to ICAD cleavage.

The SET Complex Contains a GzmA-Activated DNase and Its Inhibitor

We previously postulated that GAAD is in the SET complex since the SET complex, isolated by S-AGzmA affinity purification and gel filtration (Figure 2A), is all that is required for GzmA to activate DNA damage in isolated nuclei (Figures 2B and 2C) (Beresford et al., 2001). In vitro plasmid DNA cleavage by the SET complex is Mg^{+2} dependent and sequence independent but requires prolonged incubation (48 hr at 37°C), suggesting that the SET complex contains not only GAAD, but possibly an inhibitor (IGAAD). GzmA inactivates the inhibitor since plasmid DNase activity is detected within 2 hr if the SET

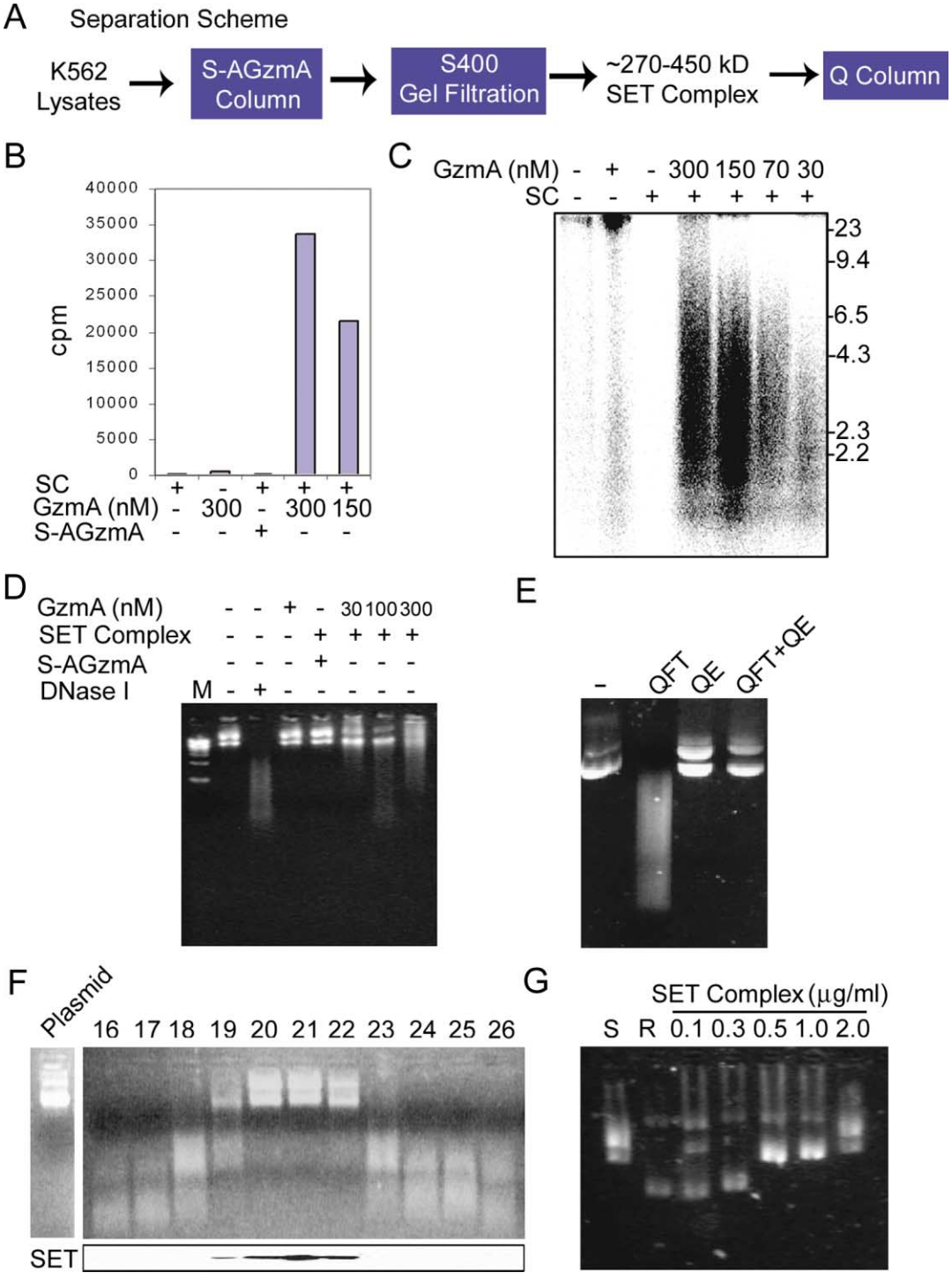

Figure 2. The SET Complex Contains GAAD and Its Inhibitor

(A) Purification scheme of GAAD. The 270–450 kDa SET complex elutes from cell lysates applied sequentially to immobilized S-AGzmA and S400 columns. The pooled S400 fractions were further separated on a Q column.

(B and C) GzmA activates nuclease activity in the SET complex (SC). Isolated Jurkat nuclei were treated with GzmA or S-AGzmA and SC and then radiolabeled with Klenow, detected by counting (B) or alkaline agarose gel electrophoresis (C).

(D) GzmA-treated SET complex induces pcDNA3 DNA degradation. S-AGzmA concentration, 0.3 μM. DNase I is the positive control. M, 1 kb DNA markers.

(E) The Q column separates a DNase in the flowthough (QFT) from an inhibitor in the eluate (QE). Plasmid DNA was incubated with QFT and/or QE. The QFT DNase was inhibited completely by the QE.

(F) The QE inhibitor coelutes from the Q column with SET. Plasmid DNA, coincubated with QFT and the indicated QE fractions, was analyzed by agarose gel electrophoresis (above). QE fractions were probed for SET (below).

(G) The SET complex reassembles topoisomerase-relaxed (R) plasmid DNA around histones into its supercoiled (S) form.

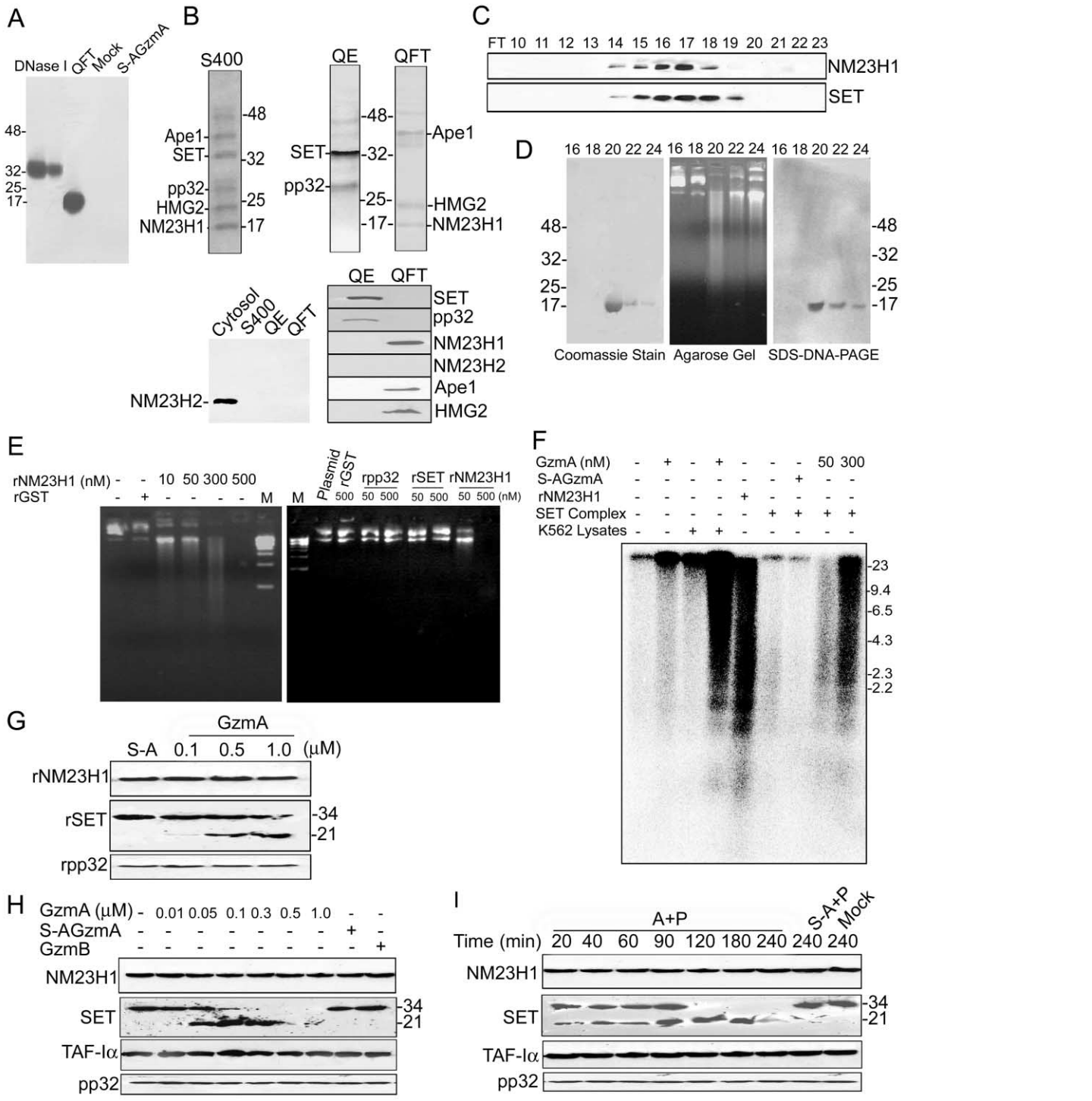

Figure 3. ER-Associated GAAD Is NM23-H1

(A) The SET complex QFT DNase, visualized by SDS-DNA-PAGE, migrates with an apparent mass of ~17 kDa. No DNase was in mock- or GzmA-treated rSET or in GzmA or rpp32 (data not shown). DNase I is a positive control.

(B) A 17 kDa band in the QFT was identified as NM23-H1 by mass spectrometry. The SET complex from the S400 column and pooled QE and QFT fractions were analyzed by Coomassie staining (above) and by immunoblot (below). SET and pp32 are in the QE. NM23-H1, Ape1, and HMG2 are in the QFT. NM23-H2 is not in the SET complex, but is detectable in cytosol.

(C) NM23-H1 coelutes from the S-AGzmA column with SET and Ape1, HMG2, and pp32 (data not shown). Immunoblot was probed with NM23-H1 mAb and SET polyclonal antiserum.

(D) rNM23-H1 has DNase activity. The rNM23-H1 fractions from the final DEAE purification step were analyzed by Coomassie staining and by EtBr-stained agarose and SDS-DNA-PAGE gels for nicking of plasmid and eukaryotic DNA, respectively.

(E) rNM23-H1 cuts plasmid DNA at nanomolar concentrations. Control recombinant GST, pp32, or SET proteins have no DNase activity.

(F) rNM23-H1 can replace GzmA-treated cytosol or SET complex to nick DNA in isolated nuclei.

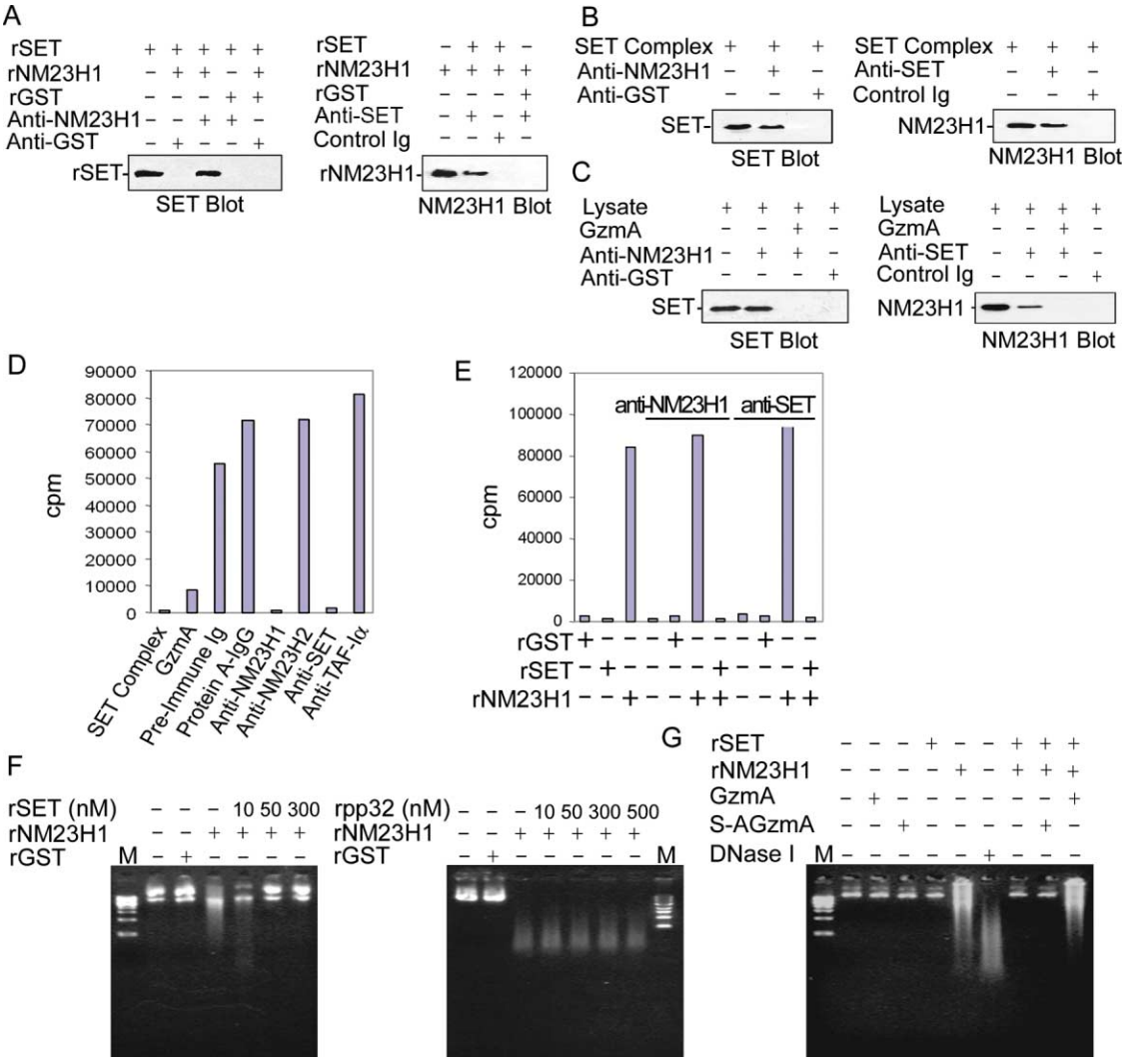

Figure 4. SET Binds and Inhibits GAAD

(A–C) rSET binds directly to rNM23-H1. rSET and rNM23-H1 were coprecipitated with NM23-H1 mAb (left) or SET antiserum (right). Native SET and NM23-H1 in the SET complex (B) or K562 cell lysates (C) also coprecipitate with antibody to NM23-H1 (left) or SET (right). Pretreating lysates with GzmA blocks coprecipitation.

(D) Immunodepletion of NM23-H1 or SET in the SET complex, but not their homologs NM23-H2 or TAF-Iα, abolishes GAAD activity. SET complex was immunodepleted with preimmune serum, protein A-purified IgG, or indicated antibodies and Protein A Sepharose (Pharmacia). Supernatants were then treated with 0.3 μM GzmA and added to isolated nuclei. DNA nicking was measured as in Figure 1A. Control lanes show no nicking in nuclei treated only with SET complex or GzmA.

(E) DNA nicking by GzmA-activated SET complex rescued after immunodepletion by adding back rNM23-H1, but not rNM23-H1 plus SET. Experiment was performed as in (D), but indicated proteins were added to supernatants just prior to adding nuclei.

(F) rSET, but not rpp32, inhibits rNM23-H1 nuclease activity.

(G) GzmA, but not S-AGzmA, releases the IGAAD activity of rSET and allows rNM23-H1 to degrade plasmid DNA. M, 1 kb DNA markers.

complex is pretreated with GzmA, but not with S-AGzmA (Figure 2D). To identify GAAD, the SET complex was separated over an anion exchange Q column. SET and pp32 bind to the Q column, while Ape1 and HMG-2 are in the flowthrough (QFT) (Figure 3B). CAD and ICAD are not in the SET complex (data not shown). The Q column eluate (QE) does not cut plasmid DNA, but the QFT does. Moreover, mixing the QE with the QFT abrogates DNA cleavage (Figure 2E). The inhibitory QE fractions coincide with the fractions that contain SET and pp32 (Figure 2F; data not shown). Inhibition is specific since the QE does not inhibit DNase I (data not shown). Therefore, GAAD is in the QFT, and IGAAD is in the QE. Moreover, the intact SET complex, like SET itself, has NAP activity,

(G–I) In (G), GzmA does not cut rNM23-H1. rNM23-H1, rSET, or rpp32, treated with GzmA or 1μM S-AGzmA, were analyzed by immunoblot. GzmA also does not degrade native NM23-H1 in K562 cell lysates (H) or when GzmA is loaded with perforin (P) into K562 cells (I). SET, but not pp32 or TAF-Iα, is cleaved under these conditions.

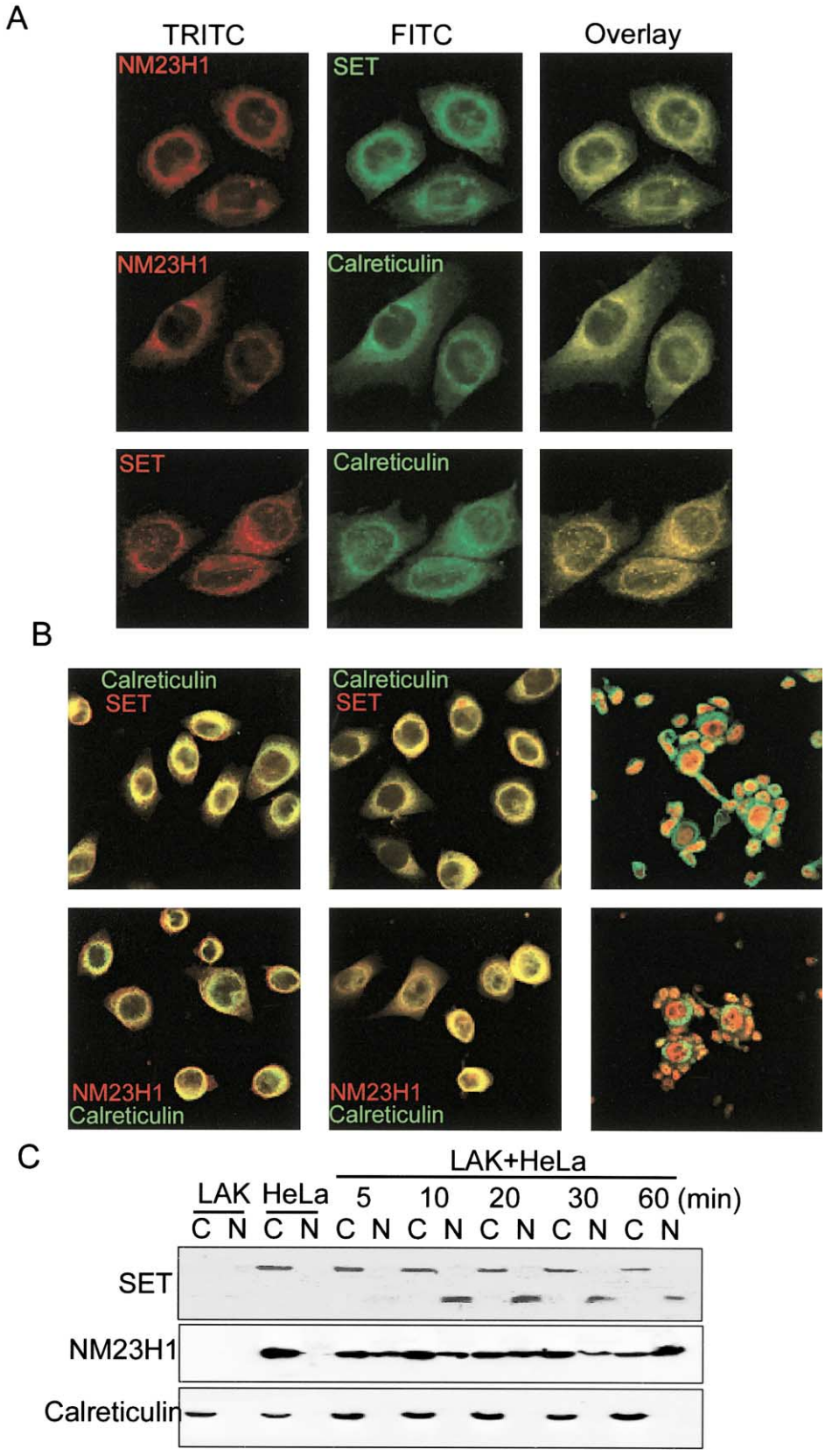

Figure 5. NM23-H1 Colocalizes with SET and Rapidly Translocates to the Nucleus after CTL Attack

(A) NM23-H1 and SET colocalize with each other and with the ER-resident protein calreticulin in HeLa cells. TRITC red fluorescence is shown at left, FITC staining green in the middle, and the merged image at right.

which is destroyed by GzmA (Beresford et al., 2001) (Figure 2G; data not shown).

SET Complex GAAD Is NM23-H1

SDS-DNA-PAGE identifies nucleases separated on gels impregnated with calf thymus DNA by EtBr-negative bands that emerge after renaturation. A 17 kDa band is in the QFT, but not in the QE, GzmA-treated QE, or recombinant QE proteins (Figure 3A; data not shown). This 17 kDa QFT protein was identified as NM23-H1 at the Harvard Microchemistry Facility by microcapillary reverse phase HPLC nanoelectrospray tandem mass spectroscopy by sequence identity of 12 tryptic fragments and confirmed by immunoblot probed with NM23-H1 mAb (Figure 3B). The association of NM23-H1 is specific, since NM23-H2 is not in the complex. NM23-H1, but not NM23-H2, also coelutes with SET and other SET complex proteins from the S-AGzmA column (Figure 3C; data not shown).

To determine whether recombinant NM23-H1 (rNM23-H1) is a DNase, rNM23-H1 protein was purified from bacteria using ammonium sulfate precipitation, hydroxyapatite, ATP agarose, and DEAE chromatography. Coomassie staining of PAGE gels of the final DEAE column elution reveals a solitary rNM23-H1 band (Figure 3D). DNase activity against plasmid and eukaryotic DNA, visualized on agarose and SDS-DNA-PAGE gels, respectively, coincides with fractions containing rNM23-H1. rNM23-H1 cleavage of plasmid DNA is dose dependent and readily detected at low nanomolar concentrations (Figure 3E). Control recombinant proteins (rGST, rSET, or rpp32) have no nuclease activity at 500 nM. The DNase activity of NM23-H1 is Mg^{+2} dependent (data not shown), like GAAD activity in the SET complex. rNM23-H1 can replace GzmA-treated cytosol or SET complex to reconstitute DNA nicking activity in isolated Jurkat nuclei, but does not require GzmA to activate it (Figure 3F).

NM23-H1 Is Not a GzmA Substrate

Since rNM23-H1 is a DNase, NM23-H1 need not be a GzmA substrate. To determine whether NM23-H1 and GzmA interact directly, we tried to coprecipitate the recombinant proteins. rNM23-H1 does not coprecipitate with S-AGzmA, although recombinant GzmA substrates SET, HMG-2, and Ape1 do (data not shown). However, native NM23-H1 in the SET complex or in cell lysates coprecipitates with S-AGzmA, suggesting an indirect interaction via other SET complex proteins (data not shown). Furthermore, a molar excess of GzmA does not cut rNM23-H1 (Figure 3G). As expected, GzmA cuts rSET, but not rpp32. These results were verified by probing for NM23-H1, SET, and pp32 in K562 cell lysates incubated with Gzms (Figure 3H) or in intact K562 cells loaded with GzmA and perforin (Figure 3I). Native NM23-H1 is unchanged 4 hr after GzmA treatment, while SET (but not its homolog TAF-Iα) is cleaved within 20 min.

SET Binds to GAAD and Is Its Inhibitor

GzmA does not activate DNA damage by cutting NM23-H1. However, GAAD might be activated by cleaving its inhibitor IGAAD, just as CAD is activated by ICAD cleavage. Since IGAAD is in the QE of the SET complex fractionation, we determined which SET complex proteins bind NM23-H1. rNM23-H1 coprecipitates with rSET, but not with rpp32, rHMG-2, or rApe1 (Figure 4A; data not shown). Native NM23-H1 and SET in the SET complex (Figure 4B) or cell lysates (Figure 4C) also coprecipitate. GzmA cleavage dissociates SET and its fragments from NM23-H1, since coprecipitation is not detected after GzmA treatment even with polyclonal SET antiserum (Figure 4C; data not shown).

As expected if SET and NM23-H1 bind, immunodepletion of NM23-H1 or SET, but not control antibody or Protein A, abolishes DNA nicking by GzmA and SET complex in isolated nuclei (Figure 4D). Depletion with antibodies to TAF-Iα or NM23-H2 does not interfere with DNA nicking, showing the specificity of SET and NM23-H1 in this process. DNA nicking after immunodepletion is rescued by adding back rNM23-H1 (Figure 4E). However, adding both rNM23-H1 and SET in equimolar amounts does not restore nicking.

Because SET binds NM23-H1 and is a GzmA substrate, we tested whether rSET inhibits the rNM23-H1 nuclease. rSET, but not rpp32, blocks plasmid degradation by NM23-H1 (Figure 4F). Inhibition is specific since rSET does not inhibit DNase I (data not shown). rpp32 does not suppress the DNase activity of NM23-H1, even in 10-fold molar excess. Therefore, SET is IGAAD. To determine whether GzmA releases SET inhibition, rNM23-H1 was incubated with rSET or GzmA-pretreated rSET prior to adding plasmid DNA. GzmA, but not S-AGzmA, treatment of rSET abrogates NM23-H1 inhibition (Figure 4G).

NM23-H1 Colocalizes with SET and Moves Rapidly to the Nucleus after CTL Attack

We previously showed that SET and pp32 are predominantly cytoplasmic and associate with the ER (Beresford et al., 2001). In HeLa cells costained for NM23-H1 and SET, NM23-H1 colocalizes with SET and the ER-resident protein calreticulin (Figure 5A). Most NM23-H1 and SET are also in the cytosol, not the nucleus, when fractionated HeLa or K562 cells are analyzed by immunoblot (Figure 5C; data not shown).

To look at changes in NM23-H1 and SET during CTL attack, lymphokine-activated killer (LAK) cells were cen-

(B) NM23-H1 and SET translocate to the nucleus of target cells immediately after LAK attack. HeLa cells were pretreated with conA (middle and right) or medium (left) in the presence of EGTA (to prevent cytotoxic granule release) before adding LAK cells (right) or medium (left, middle). Cells were fixed 5 min after adding $CaCl_2$ to initiate LAK cell granule exocytosis. Calreticulin is stained green; SET (top) and NM23-H1 (bottom) are red. All images are merged. The small cells in the right figures are LAK cells. SET also translocates to the nucleus in LAK cells.

(C) Nuclear translocation of NM23-H1 and SET after LAK attack of HeLa cells (as in [B]) assessed by immunoblot of cytoplasmic (C) and nuclear (N) NP40 cell lysates. NM23-H1 and SET are mostly in the cytosol in mock-treated cells and translocate within 5 min of LAK attack. NM23-H1 is not degraded. Cleaved SET is only detected in the nucleus. Calreticulin is a loading and fractionation control.

trifuged onto concanavalin A (ConA)-treated HeLa targets in medium containing EGTA to prevent granule exocytosis. After adding Ca^{+2} to initiate cytolysis, slides were fixed and stained for NM23-H1, SET, and calreticulin (Figure 5B). Within 5 min, NM23-H1 and SET translocate from the cytoplasm to the nucleus of target cells and stain the nucleoplasm diffusely, avoiding the nucleolus. Adding just calcium to ConA-treated or untreated HeLa cells does not induce significant translocation. Of note, SET also moves to the nucleus of LAK cells within 5 min of adding Ca^{+2}. The signal for NM23-H1 in LAK cells is harder to delineate but does not appear to change within the first 5 min.

Changes in NM23-H1 and SET were also analyzed by immunoblot of cytosolic and nuclear fractions of target-LAK cell mixtures obtained in the hour after LAK attack (Figure 5C). Most NM23-H1 and SET is in HeLa cytosol before attack. LAK cell NM23-H1 or SET is not detected when equal numbers of LAK and HeLa cells are loaded, either because of lower expression or because LAK cells are much smaller. Therefore, blots of the cell mixtures detect NM23-H1 and SET in the targets. Within 5 min, the SET cleavage fragment is detected (only in the nucleus) and increases over 20 min. Cytosolic full-length SET declines with time, but the cleavage fragment is not seen in the cytosol. Therefore, either the cleaved fragment moves rapidly to the nucleus or most SET cleavage occurs after translocation. NM23-H1 translocation to the target cell nucleus occurs with similar kinetics, but NM23-H1 is not degraded. Calreticulin, a control for fractionation and loading, is unchanged. Similar results were found after loading GzmA and perforin into K562 cells (data not shown).

Silencing NM23-H1, but Not NM23-H2, Decreases GzmA-Induced DNA Nicks

As further evidence that NM23-H1 is a GAAD, NM23-H1 expression was silenced using RNA interference (RNAi) (Elbashir et al., 2001). Two siRNA duplexes targeting NM23-H1 were transfected into K562 cells. Three days later, NM23-H1 expression is not detected in cells transfected with either siRNA duplex, while cells transfected with control siRNA targeting GFP have unchanged NM23-H1 expression (Figure 6A). Cells with silenced NM23-H1 expression have many fewer DNA breaks (measured by Klenow labeling) after GzmA treatment of cell lysates compared to cells treated with GFP-siRNA (mean 10^5 cpm in NM23-H1 versus GFP-silenced cells: siRNA#1, 1.4 ± 0.1 versus 4.2 ± 0.1, $p < 0.001$; siRNA#2, 1.6 ± 0.1 versus 4.5 ± 0.2, $p < 0.001$) (Figure 6B). NM23-H1 silencing also interferes with GzmA-mediated cytolysis. When GzmA is loaded with perforin into ^{51}Cr-labeled HeLa cells 3 days after transfection, HeLa cells with silenced NM23-H1 are nearly twice as resistant to GzmA-induced cytolysis as GFP-silenced cells (specific cytotoxicity, $48\% \pm 4\%$ versus $79\% \pm 6\%$, $p < 0.001$). There are no substantial differences in background lysis ($<10\%$) by GzmA or perforin alone or by perforin and S-AGzmA due to siRNAs. Because NM23-H1 silencing does not completely abrogate DNA nicking, we cannot be certain that NM23-H1 is the only GAAD. However, RNAi does not usually completely abolish targeted gene expression.

The siRNAs chosen to silence NM23-H1 do not alter NM23-H2 expression (Figure 6A). To verify that the NM23-H1 homolog NM23-H2 is not involved in GzmA-mediated DNA damage, we also tested whether DNA nicking is reduced in NM23-H2-silenced cells (Figure 6C). NM23-H2 was not detected by immunoblot in cells transfected 3 days earlier with siRNA duplex #1, while siRNA#2 inhibited NM23-H2 expression by $\sim$60%. NM23-H2-silenced cells have comparable GzmA-induced nicking as control cells (mean 10^5 cpm in NM23-H2 versus GFP-silenced cells: siRNA#1, 2.7 ± 0.1 versus 3.0 ± 0.1, $p > 0.05$; siRNA#2, 3.1 ± 0.2 versus 2.9 ± 0.2, $p > 0.05$).

Overexpressing NM23-H1 Enhances GzmA-Induced DNA Breaks

To validate further the role of NM23-H1 in GzmA-induced DNA damage and cell death, NM23-H1 was overexpressed by transfection with pCMV-NM23-H1. Cells transfected with NM23-H1, but not control, plasmid have a dose-dependent increase in NM23-H1 expression (Figure 6D), which parallels increased GzmA-initiated nicking (Figure 6E). Cells overexpressing NM23-H1 are also more susceptible than GFP-transfected cells to GzmA and perforin-mediated cytolysis (specific cytotoxicity, $91\% \pm 7\%$ versus $65\% \pm 5\%$, $p < 0.001$). However, when NM23-H2 is overexpressed, GzmA-induced DNA nicking is unaltered (Figure 6F).

Silencing SET Enhances and Overexpressing SET Diminishes GzmA-Induced DNA Nicks

To verify the role of SET as IGAAD, SET was silenced using siRNAs designed to target SET, but not its close homolog TAF-Iα. Transfection of siRNA#1 inhibits SET expression by $\sim$60%, while siRNA#2 blocks expression almost completely; neither interferes with TAF-Iα (Figure 6G). Cells with silenced SET expression are more sensitive to GzmA-induced DNA breaks compared to cells treated with GFP-siRNA, and DNA damage increases with more complete silencing (mean 10^5 cpm in SET-silenced versus GFP-silenced cells: siRNA#1, 3.5 ± 0.2 versus 2.2 ± 0.2, $p < 0.001$; siRNA#2, 4.8 ± 0.3 versus 2.5 ± 0.2, $p < 0.001$) (Figure 6G).

Overexpressing SET in K562 cells by transfecting pcDNA3.1-SET also leads to a dose-dependent increase in SET expression and a corresponding decrease in GzmA-induced DNA breaks (Figure 6H). The mean 10^5 cpm in SET-overexpressing versus GFP-overexpressing cells was: 3.1 ± 0.2 versus 3.4 ± 0.05, $p < 0.01$ (0.2 μg DNA); 1.8 ± 0.2 versus 3.7 ± 0.2, $p < 0.001$ (0.4 μg); and 1.3 ± 0.2 versus 3.6 ± 0.2, $p < 0.001$ (0.8 μg). These experiments with altered SET expression confirm the inhibitory role of SET in DNA damage by GzmA.

Discussion

GzmA was thought to activate cell death slowly because oligonucleosomal DNA fragments are not released from target cells until 16 hr after GzmA treatment. However, GzmA activates a type of DNA damage (single-stranded nicks), which leads to larger DNA fragments, not detected in conventional apoptotic assays using nondenaturing agarose gels or TdT labeling. Nonetheless, DNA

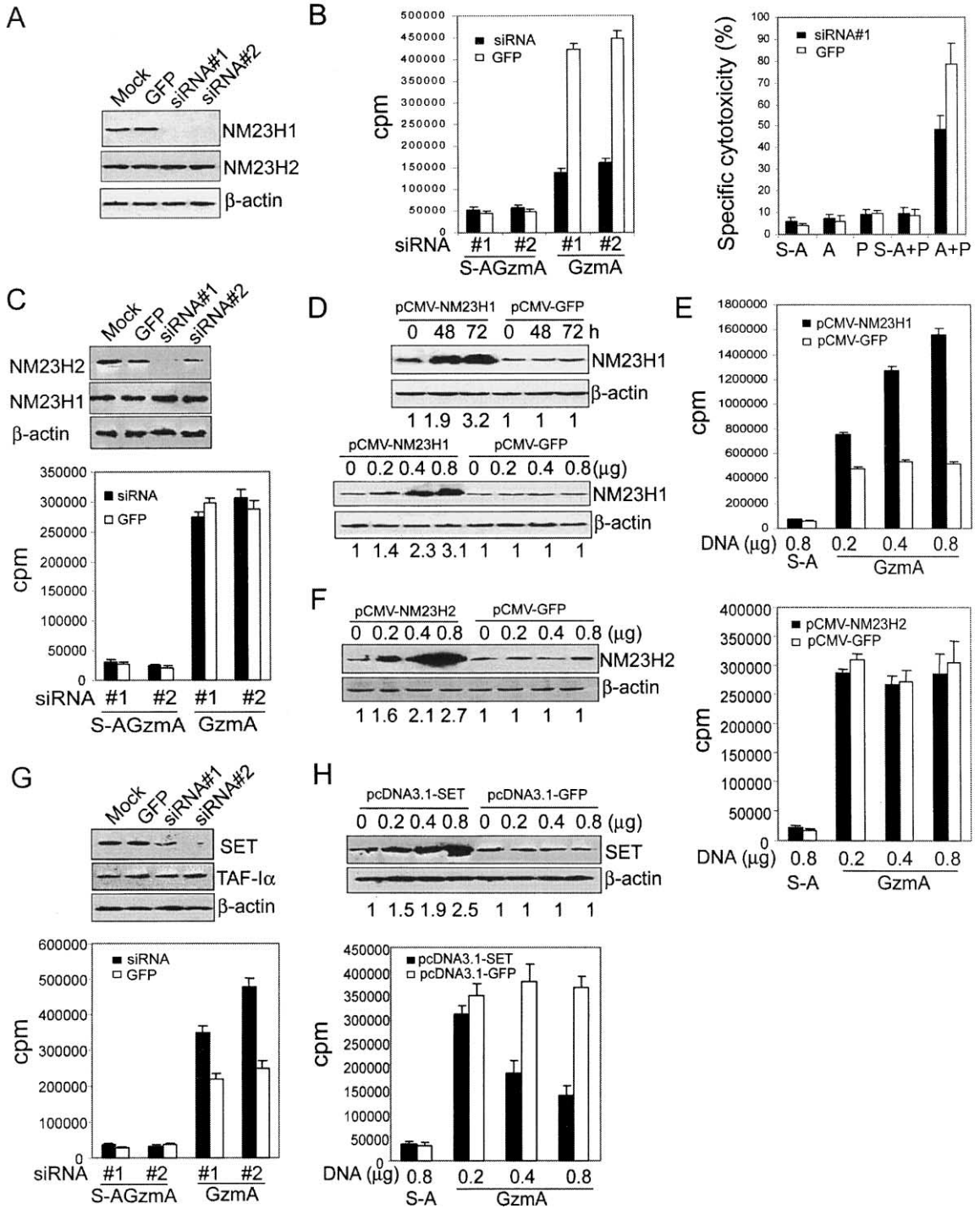

Figure 6. Silencing NM23-H1 Expression Decreases and Overexpressing NM23-H1 Enhances GzmA-Induced DNA Damage

(A) NM23-H1 expression is silenced in HeLa cells after treatment with siRNA duplexes against NM23-H1. NM23-H2 and β-actin expression are unchanged.

(B) Silencing NM23-H1 significantly decreases GzmA-induced DNA damage, measured as in Figure 1A, and cytolysis of perforin and GzmA-loaded cells.

(C) Silencing NM23-H2 does not affect DNA nicking activated by GzmA.

(D and E) HeLa cells transfected with pCMV-NM23-H1, but not control plasmid pCMV-GFP, overexpress NM23-H1 in a plasmid dose-dependent manner. Blots of cell lysates were probed for NM23-H1 and β-actin. Numbers represent the ratio of NM23-H1 to β-actin signal by densitometry, normalized to control cells. NM23-H1 overexpression enhances GzmA-mediated DNA nicks in parallel with NM23-H1 expression (E).

(F) Overexpressing homologous NM23-H2 has no effect on DNA nicking.

(G and H) Silencing SET enhances (G), while overexpressing SET diminishes (H), GzmA-induced DNA damage.

damage occurs within 4 hr and can be detected in situ and in vitro by labeling single-stranded nicked DNA with Klenow. Moreover, GzmA-induced cell death occurs within minutes, as rapidly as with GzmB (data not shown). Although these results are not completely physiological since they are obtained using recombinant granzymes and purified perforin, it is likely that the same kinetics occur after CTL granule release. However, the kinetics of granzyme A-mediated cell death in a more physiologically relevant setting require further study, which should be possible with CTLs from mice genetically deficient in granzyme B.

Granzyme A-induced cell death is marked by rapid induction of other apoptotic features, including loss of membrane integrity with blebbing, loss of mitochondrial potential, and production of reactive oxidative species (D.M. and J.L., unpublished), chromatin condensation, and nuclear fragmentation (Beresford et al., 1999; Fan et al., 2003). However, the biochemical hallmarks of the caspase pathway, such as mitochondrial cytochrome c release, oligonucleosomal DNA fragmentation, caspase activation, and inhibition by bcl-2 overexpression, are absent (Beresford et al., 1999). Moreover, the known GzmA intracellular targets (SET, HMG-2, Ape1, lamins A–C, and histones) are (with the exception of lamin B) all unique to this pathway (Beresford et al., 1997; Fan et al., 2002, 2003; Zhang et al., 2001a, 2001b). This pathway therefore provides an immune mechanism to eliminate tumors and viruses that can evade caspase-mediated apoptosis.

GzmA targets the SET complex, which contains pp32 and three GzmA substrates, SET, HMG-2, and Ape1 (Beresford et al., 1997; Fan et al., 2002, 2003). We now show that the SET complex holds the key to the unique DNA damage induced by GzmA. A new SET complex component is NM23-H1, an evolutionarily conserved NDP kinase previously known to nick DNA (Ma et al., 2002). NM23-H1 is a GAAD, and SET is its inhibitor. GzmA activates the DNase by cleaving SET, disrupting its binding to NM23-H1 and releasing it from inhibition (Figure 7). This mechanism recalls the activation of CAD by caspase or GzmB cleavage of ICAD. In both pathways, the DNase is sequestered in the cytosol bound to its inhibitor, until the inhibitor is proteolytically cleaved. During cell death, the uninhibited DNase translocates to the nucleus.

The signals that regulate SET complex nuclear translocation are unknown. However, the functions of these proteins suggest they should spend time in the nucleus. In this study, SET and NM23-H1 in target cells move to the nucleus within minutes of GzmA loading. Although the SET fragment is only seen in the nucleus, further experiments are required to determine whether SET is cleaved only in the nucleus or whether SET fragments produced in the cytosol are not detected there because they are unstable or rapidly translocate.

GzmA translocates to the nucleus during CTL attack (Fan et al., 2003; Jans et al., 1999), although how GzmA gets in is not known. Possibly, one of the SET complex proteins is involved in its transport. pp32, which has nuclear import and export sequences (Brennan et al., 2000), also translocates with SET (P.J.B. and J.L., unpublished data) and Ape1 also concentrates in the nucleus within minutes of GzmA loading (Fan et al., 2003).

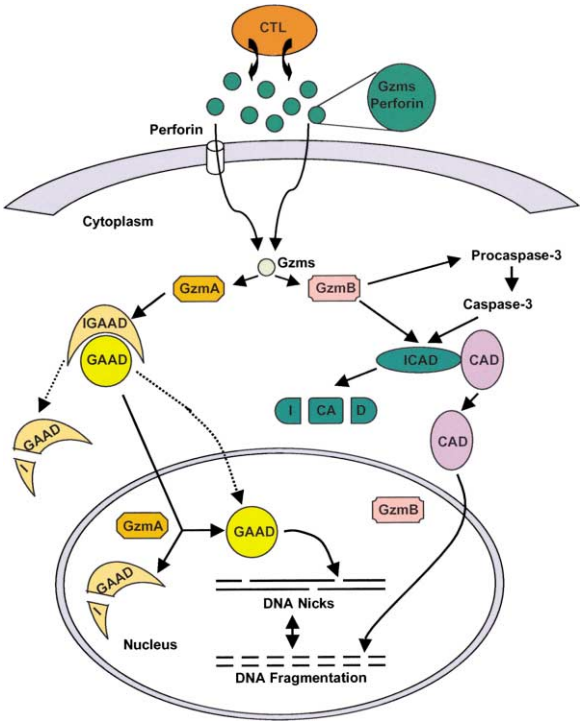

Figure 7. Model for DNA Damage during CTL-Mediated Apoptosis

CTL granules containing perforin and granzymes are released into the synapse formed with the target cell. Gzms enter the target cell cytoplasm either via perforin-induced perturbation of the plasma membrane or through endocytosis. GzmA cleaves IGAAD (SET), which then no longer binds and inhibits GAAD (NM23-H1). Our experiments do not define whether SET is cleaved in the cytoplasm or nucleus or both. Uninhibited GAAD in the nucleus makes single-stranded DNA nicks. GzmB directly or indirectly via caspases destroys the CAD inhibitor ICAD. Cleaved ICAD no longer binds CAD, which then moves to the nucleus to cause double-stranded breaks.

Moreover, Ape1 translocates rapidly into the nucleus in response to ROS generated during GzmA-induced cell death (Tell et al., 2000). Therefore, we suspect that the SET complex translocates as a complex in response to GzmA loading, although this remains unproven. Of note, SET (but maybe not NM23-H1) also moves to the nucleus of LAK cells activated to lyse target cells (Figure 5B). This result suggests that SET may play a role in nuclear events in cellular activation. In fact, SET has been postulated to link transcriptional activation with histones (Seo et al., 2001; Shikama et al., 2000).

NM23-H1 was identified on the basis of low expression in metastatic cells (Steeg et al., 1988). Since then, low expression or mutation of NM23-H1 and NM23-H2 have been implicated in cancer prognosis or metastasis in a variety of tumors and malignant transformation. However, how NM23 proteins enhance malignancy is not completely understood. Most NM23 family members are NDP kinases (reviewed in Lascu, 2000). NDP kinases were originally thought of as essential housekeeping enzymes required for maintaining NTP pools. However, NDP kinase is not essential for viability in *E. coli* and in yeast. Deletion of the *ndk* gene in *E. coli* produces a mutator phenotype, suggesting DNA repair defects (Lu et al., 1995; Postel et al., 2000), and a deficient strain in *S.*

pombe has developmental abnormalities (Izumiya and Yamamoto, 1995). The close homolog NM23-H2 was first identified as a DNA binding protein that enhances *c-myc* transcription (Postel et al., 1993). However, DNA binding and NDP kinase activity are controlled by independent functional domains of NM23-H2 (Postel et al., 1996). NM23-H2 preferentially binds to paranemic DNA structures and nicks the *c-myc* NHE promoter through a covalent protein DNA complex involving a DNA glycosylase/lyase reaction (Postel et al., 2000). Perhaps DNA nicking involves NM23 transfer of a phosphoryl group to DNA. Mutational and structural analysis implicate seven critical NM23-H2 residues for covalent DNA binding, DNA cleavage, and NDP kinase activity (Postel et al., 2002). These seven residues are conserved between NM23-H1 and NM23-H2, indicating that NM23-H1 may have similar activities as NM23-H2. In fact, NM23-H1 represses *PDGF-A* transcription and nicks the *PDFG-A* 5′-SHS silencer and NHE basal promoter (Ma et al., 2002). Although both NM23-H1 and NM23-H2 nick DNA, their cleavage recognition sites and mechanisms appear to be different. In this study, NM23-H1, but not NM23-H2, is in the SET complex and plays a role in GzmA-mediated death.

How does the inclusion of NM23-H1 in the SET complex and its role as GAAD help us understand the normal function of NM23-H1 and the SET complex? First, this study confirms that NM23-H1 has DNA nicking activity. Its coassociation with Ape1, the rate-limiting enzyme in BER, suggests that NM23-H1 may act as a DNA glycosylase/lyase in concert with Ape1 in repairing oxidative DNA damage, since glycosylases are the first step in BER. Disruption of DNA repair might explain why loss of *ndk* in *E. coli* leads to a mutator phenotype and why NM23-H1 is heavily implicated in cancer prognosis. Loss of NM23-H1 expression in tumors might also make them resistant to immune surveillance by CTL and NK cells, since target cells with silenced NM23-H1 are less sensitive to GzmA-induced cell death. In the SET complex HMG-2, which preferentially recognizes distorted DNA structures including single-stranded DNA, may help target NM23-H1 and Ape1 to damaged DNA in need of repair and to paranemic regions of DNA implicated in transcriptional regulation. The NAP activity of SET might also play a role in making nucleosomal DNA accessible to repair and/or transcriptional activation. There have been no studies of the influence of chromatin structure on BER. However, damaged DNA in activating transcribed genes (with more open chromatin) is preferentially repaired (Bohr et al., 1985). In fact, a DNA oligonucleotide containing a T(6-4)T photoproduct was repaired ten times less efficiently in nucleosomal DNA than in naked DNA (Hara et al., 2000). Apparently, under normal circumstances, the nicks initiated by NM23-H1 are quickly repaired (perhaps using Ape1). However, during GzmA-mediated cell death, Ape1 is a GzmA substrate, and its cleavage leads to loss of function. Therefore, GzmA hijacks a DNA repair pathway and converts it to induce DNA damage.

The SET complex proteins are implicated not only in DNA repair, but also in transcription. SET binds CBP/p300 and inhibits histone acetylation and DNA demethylation (Cervoni et al., 2002; Seo et al., 2001, 2002; Shikama et al., 2000). Ape1 reduces oxidized transcription factors involved in the immediate early gene response, including fos, jun, NF-κB, and p53 (Gaiddon et al., 1999; Xanthoudakis et al., 1992). The simplest model tying all these known functions together is that the SET complex is involved in repair and transcriptional activation in response to oxidative stress. The SET complex appears to move into the nucleus rapidly in response to ROS. Oxidative stress might also accompany normal cellular activation because of enhanced cellular metabolism. This might explain SET translocation even in LAK cells not threatened with death. Moreover, coupling DNA repair to transcription, recently described in other pathways (Monteiro 2000), is an efficient way to guarantee that DNA is repaired before the activated cell replicates DNA.

Chromatin degradation in apoptosis may involve more than one endonuclease. During apoptosis, genomic DNA is initially cut to 50–300 kb fragments followed by ultimate degradation to 180–200 bp oligonucleosomal fragments (Kokileva, 1994; Lagarkova et al., 1995). The last step involves the caspase-activated DNase (CAD) and, possibly, mitochondrial endoG (Enari et al., 1998; Li et al., 2001; Liu et al., 1997). CAD shows weaker nuclease activity on naked DNA than chromosomal DNA, suggesting that CAD may require other factors for optimal activity (Toh et al., 1998). In fact, CAD activity is enhanced by the SET complex protein HMG-2 and a recently described helicase (Kovacsovics et al., 2002). Until now, no other DNase responsible for DNA nicking in apoptosis has been identified. However, IGAAD is not cleaved by GzmB or during caspase-mediated apoptosis. Moreover, CAD and ICAD are not in the SET complex. Therefore the SET complex is probably not involved during caspase activation. However, serine protease inhibitors block caspase-mediated apoptosis (Weaver et al., 1993). An unknown endogenous serine protease may, therefore, activate a DNA nicking enzyme as a first step in caspase DNA degradation. However, during CTL and NK cell killing, NM23-H1 may nick DNA into large fragments before CAD-triggered oligonucleosomal DNA fragmentation. This might contribute to the synergy of GzmA and GzmB in degrading chromatin (Beresford et al., 1999; Nakajima et al., 1995).

Experimental Procedures

Cell Lines and Antibodies

K562, Jurkat, and HeLa cells (ATCC) were grown in RPMI1640 with 10% FCS, 2 mM glutamine, 2 mM HEPES, 100 units/ml penicillin, 100 mg/ml streptomycin, and 50 μM β-mercaptoethanol. Mouse pp32 mAb (RJ1) and SET rabbit antiserum were described (Beresford et al., 2001). Mouse SET and TAF-Iα mAbs were kind gifts of K. Nagata (Nagata et al., 1998). Commercial antibodies were rabbit antisera against CAD (Molecular Biologische Technologie); ICAD, HMG-2 (BD PharMingen); Ape1, NM23-H1, NM23-H2 (Santa Cruz); calreticulin (Stressgen Biotech Corp.); and GST (Clontech); mouse mAb against NM23-H1 (BD PharMingen) and β-actin (Sigma-Aldrich); and HRP-conjugated sheep anti-mouse IgG, HRP-conjugated monkey anti-rabbit IgG (Amersham), FITC-conjugated goat anti-rabbit IgG (Zymed), and TRITC-conjugated goat anti-mouse IgG (Molecular Probes). Coprecipitation and immunoblot were performed as described (Fan et al., 2003).

Recombinant Proteins, Expression Plasmids, and Purified Perforin

GzmA and GzmB and inactive S-A mutants were expressed and purified as previously reported (Beresford et al., 1999). Perforin was

purified from rat RNK-16 cells, and cells were loaded with Gzms using a sublytic concentration of perforin as described (Shi et al., 1992). pp32, SET, and GST were expressed in BL21-DE3 cells and purified as described (Zhang et al., 2001b). Recombinant NM23-H1 was purified by ammonium sulfate precipitation followed by hydroxyapatite, ATP agarose, and DEAE ion exchange (Pharmacia) fractionation using NM23-H1 expressed from pet 15b, a kind gift of P. Steeg (National Institutes of Health, USA). Mammalian expression plasmids for NM23-H1 and NM23-H2 cDNA in pCMV were kind gifts of P. Steeg and E. Postel (Princeton University), respectively. SET was cloned into pcDNA3.1 for transfection experiments.

Purification of SET Complex and DNase

The SET complex was eluted from a S-AGzmA column loaded with K562 cell lysates as described (Fan et al., 2003). The concentrated desalted eluate was applied in Tris-buffered saline to a Sephacryl 400 gel filtration (2.5 cm × 1.0 m; Pharmacia). The pooled S400 fractions were concentrated, desalted, and separated on a 2 ml anion exchange Q column (Pharmacia) eluted with 0–1 M NaCl.

DNA Nicking Assay

The Klenow fragment of DNA polymerase (New England Biolabs) labeled DNA breaks as described (Beresford et al., 1999). NP40 cell lysates were treated with Gzms at 37°C for 4 hr and then nuclei isolated by centrifugation were washed before labeling. For some experiments, isolated untreated nuclei were incubated directly with indicated combinations of 5 μg of purified SET complex and recombinant proteins for 4 hr at 37°C. Unless otherwise indicated, concentrations were 0.2 μM for rSET, rNM23-H1, or rGST, and 1 μM for Gzms. For immunodepletion, the SET complex was treated with 5 μg indicated antibodies and Protein A Sepharose before adding Gzms. For rescue, 50 nM rGST, rSET, and/or rNM23H1 was added to the immunodepleted supernatants. Washed nuclei were labeled with Klenow and ^{32}P-dATP and analyzed by scintillation counting or alkaline gel electrophoresis as described (Beresford et al., 1999).

In Situ Nicking Assay

Isolated K562 nuclei were treated for 90 min at 37°C with combinations of 0.5 μM GzmA or S-AGzmA, 10 U DNase I (New England Biolabs), and K562 cytosol (2×10^4 cell equivalents) in 100 μl 50 mM Tris-HCl (pH 7.9); 50 μg/ml BSA; 5 mM $MgCl_2$; 10 mM β-mercaptoethanol; 4 U Klenow; 100 μM dATP, dCTP, and dGTP; and 16 μM Alexa 568-12-UTP (Molecular Probes), adapting the method of Krystosek, 1999. Nuclei were then plated onto polyLys-coated slides and fixed and permeabilized using the Fix-and-Perm kit (Caltag Laboratories). After washing with PBS, slides were counterstained with 0.05 μg/ml SYTOX Green (Molecular Probes), washed again, and mounted with ProLong Antifade medium (Molecular Probes). Images were acquired with a Bio-Rad Radiance 2000 laser-scanning confocal microscope.

Plasmid DNA Digestion and Nucleosome Assembly Assay

Plasmid pcDNA3.1 (0.5 μg) was incubated in 20 μl of Tris-HCl (pH 7.5), 1 mM EGTA, 5 mM $MgCl_2$, and 1 mg/ml BSA at 37°C for 2 hr with 10 μl of the indicated chromatography fractions, SET complex, NM23-H1, or DNase I before deproteinization and analysis on agarose gels as described (Beresford et al., 2001). Nucleosome assembly assay was performed as described (Beresford et al., 2001), using pcDNA3.1 plasmid and indicated concentrations of SET complex instead of rSET.

SDS-DNA-PAGE

SDS-DNA-PAGE assays were performed as described (Beresford et al., 2001). Briefly, SDS-polyacrylamide gels were impregnated with calf thymus DNA. DNase activity of electrophoresed samples was assessed by EtBr staining after incubation with 1 mM EGTA, and 5 mM $MgCl_2$. To detect DNase I activity, gels were incubated for an additional 4 hr in the presence of $CaCl_2$.

Laser Scanning Confocal Microscopy

HeLa cells on collagen-coated slides were fixed, permeabilized, stained, and visualized as described (Beresford et al., 2001). For LAK attack, HeLa cells were incubated with 5 μg/ml ConA (ICN Pharmaceuticals) for 1 hr at 37°C. After washing with PBS, 100 μl culture medium containing 1 mM EGTA was added to each chamber. LAK cells (generated from human PBMCs cultured for 14 days in medium containing 1000 IU/ml recombinant human IL-2 (a gift of Chiron Oncology) added in 100 μl of medium containing 1 mM EGTA onto ConA-sensitized target cells (at a ratio of 40:1 for microscopy and 1:1 for immunoblot) were incubated for 15 min at 37°C, briefly centrifuged onto the targets, and incubated for another 15 min at 37°C. Adding $CaCl_2$ to a final concentration of 5 mM triggered granule exocytosis. Slides were returned to 37°C, and reactions were stopped at indicated times by adding fixation buffer. Samples were either lysed in NP40 lysis buffer to obtain nuclear and cytoplasmic fractions or were stained and analyzed by microscopy as above.

In Vitro Cleavage Assay

Recombinant proteins (0.5 μM) or K562 cell lysates (2×10^5 cell equivalents) were incubated for the indicated times at 37°C with indicated concentrations of Gzms in 20 μl of 50 mM Tris-HCl (pH 7.5), 1 mM $CaCl_2$, and 1 mM $MgCl_2$. Reaction products were electrophoresed and transferred to nitrocellulose for immunoblot.

Silencing by RNAi

Silencing using synthetic 21 nucleotide siRNA duplexes was performed as described (Fan et al., 2003). Synthetic siRNAs (Dharmacon Research) were as follows: NM23-H1 siRNA#1: sense 5′-GGAUUCCGCCUUGUGGGUCUU-3′, antisense 5′-GACCCACAAGG CGGAAUCCUU-3′; #2 sense 5′-UACAUGCACUCAGGGCCGGUU-3′, antisense 5′-CCGGCCCUGAGUGCAUGUAUU-3′; NM23H2: #1 sense 5′-GGGAUUCCGCCUCGUGGCCUU-3′, antisense 5′-GGCCA CGAGGCGGAAUCCCUU-3′; #2 sense 5′-GUACAUGAACUCAGGG CCGUU-3′, antisense 5′-CGGCCCUGAGUUCAUGUACUU-3′; SET: #1 sense 5′-GGAGCUCAACUCCAACCACUU-3′; antisense 5′-GUG GUUGGAGUUGAGCUCCUU-3′; #2 sense 5′-GGCCGACGAGACCU CAGAAUU-3′, antisense 5′-UUCUGAGGUCUCGUCGGCCUU-3′. GFP siRNA sequences were previously described (Fan et al., 2003). K562 cells were analyzed 3 days after transfection by immunoblot for protein expression and by cytotoxicity assay after loading with granzyme and perforin. Transfected cell lysates were also treated with Gzms to analyze DNA nicking as described above.

Overexpression of NM23-H1, NM23-H2, and SET

K562 cells, transfected with pCMV or pcDNA3.1 expression plasmids 3 days earlier as described (Fan et al., 2003), were analyzed by immunoblot and DNA nicking assay as described for silenced cells.

Acknowledgments

This work was supported by NIH Grant AI45587 (J.L.). We thank Z. Xu for technical support, L. Shi for helpful discussions, P. Steeg for NM23-H1 plasmids, E. Postel for NM23-H2 plasmid and critical review of the manuscript, K. Nagata for SET and TAF-Iα antibodies, and C. Novina for GFP siRNA.

Received: October 15, 2002
Revised: January 28, 2003

References

Bai, J., Brody, J.R., Kadkol, S.S., and Pasternack, G.R. (2001). Tumor suppression and potentiation by manipulation of pp32 expression. Oncogene *20*, 2153–2160.

Beresford, P.J., Kam, C.M., Powers, J.C., and Lieberman, J. (1997). Recombinant human granzyme A binds to two putative HLA-associated proteins and cleaves one of them. Proc. Natl. Acad. Sci. USA *94*, 9285–9290.

Beresford, P.J., Xia, Z., Greenberg, A.H., and Lieberman, J. (1999). Granzyme A loading induces rapid cytolysis and a novel form of DNA damage independently of caspase activation. Immunity *10*, 585–594.

Beresford, P.J., Zhang, D., Oh, D.Y., Fan, Z., Greer, E.L., Russo, M.L., Jaju, M., and Lieberman, J. (2001). Granzyme A activates an endoplasmic reticulum-associated caspase-independent nuclease

to induce single-stranded DNA nicks. J. Biol. Chem. *276*, 43285–43293.

Bohr, V.A., Smith, C.A., Okumoto, D.S., and Hanawalt, P.C. (1985). DNA repair in an active gene: removal of pyrimidine dimers from the DHFR gene of CHO cells is much more efficient than in the genome overall. Cell *40*, 359–369.

Brennan, C.M., Gallouzi, I.E., and Steitz, J.A. (2000). Protein ligands to HuR modulate its interaction with target mRNAs in vivo. J. Cell Biol. *151*, 1–14.

Cervoni, N., Detich, N., Seo, S.B., Chakravarti, D., and Szyf, M. (2002). The oncoprotein Set/TAF-1beta, an inhibitor of histone acetyltransferase, inhibits active demethylation of DNA, integrating DNA methylation and transcriptional silencing. J. Biol. Chem. *277*, 25026–25031.

Elbashir, S.M., Harborth, J., Lendeckel, W., Yalcin, A., Weber, K., and Tuschl, T. (2001). Duplexes of 21-nucleotide RNAs mediate RNA interference in cultured mammalian cells. Nature *411*, 494–498.

Enari, M., Sakahira, H., Yokohama, H., Okawa, K., Iwamatsu, A., and Nagata, S. (1998). A caspase-activated DNase that degrades DNA during apoptosis, and its inhibitor ICAD. Nature *391*, 43–50.

Fan, Z., Beresford, P.J., Zhang, D., and Lieberman, J. (2002). HMG2 Interacts with the nucleosome assembly protein SET and is a target of the cytotoxic T-lymphocyte protease granzyme A. Mol. Cell. Biol. *22*, 2810–2820.

Fan, Z., Beresford, P.J., Zhang, D., Xu, Z., Novina, C.D., Yoshida, A., Pommier, Y., and Lieberman, J. (2003). Cleaving the oxidative repair protein Ape1 enhances cell death mediated by granzyme A. Nat. Immunol. *4*, 145–153.

Gaiddon, C., Moorthy, N.C., and Prives, C. (1999). Ref-1 regulates the transactivation and pro-apoptotic functions of p53 in vivo. EMBO J. *18*, 5609–5621.

Hara, R., Mo, J., and Sancar, A. (2000). DNA damage in the nucleosome core is refractory to repair by human excision nuclease. Mol. Cell. Biol. *20*, 9173–9181.

Izumiya, H., and Yamamoto, M. (1995). Cloning and functional analysis of the ndk1 gene encoding nucleoside-diphosphate kinase in Schizosaccharomyces pombe. J. Biol. Chem. *270*, 27859–27864.

Jans, D.A., Sutton, V.R., Jans, P., Froelich, C.J., and Trapani, J.A. (1999). BCL-2 blocks perforin-induced nuclear translocation of granzymes concomitant with protection against the nuclear events of apoptosis. J. Biol. Chem. *274*, 3953–3961.

Kokileva, L. (1994). Multi-step chromatin degradation in apoptosis. Int. Arch. Allergy Immunol. *105*, 339–343.

Kovacsovics, M., Martinon, F., Micheau, O., Bodmer, J.L., Hofmann, K., and Tschopp, J. (2002). Overexpression of Helicard, a CARD-containing helicase cleaved during apoptosis, accelerates DNA degradation. Curr. Biol. *12*, 838–843.

Krystosek, A. (1999). Preferential sites of early DNA cleavage in apoptosis and the pathway of nuclear damage. Histochem. Cell Biol. *111*, 265–276.

Lacombe, M.L., Milon, L., Munier, A., Mehus, J.G., and Lambeth, D.O. (2000). The human Nm23/nucleoside diphosphate kinases. J. Bioenerg. Biomembr. *32*, 247–258.

Lagarkova, M.A., Iarovaia, O.V., and Razin, S.V. (1995). Large-scale fragmentation of mammalian DNA in the course of apoptosis proceeds via excision of chromosomal DNA loops and their oligomers. J. Biol. Chem. *270*, 20239–20241.

Lascu, I. ed. (2000). MINIREVIEW SERIES Nucleoside Diphosphate Kinases: Structure, Mechanism, Genetics, and Roles in Cell Metabolism, Signal Transduction, Development and Disease. J. Bioenerg. Biomemb. *32*, 211–324.

Li, L.Y., Luo, X., and Wang, X. (2001). Endonuclease G is an apoptotic DNase when released from mitochondria. Nature *412*, 95–99.

Li, M., Makkinje, A., and Damuni, Z. (1996). Molecular identification of I1PP2A, a novel potent heat-stable inhibitor protein of protein phosphatase 2A. Biochemistry *35*, 6998–7002.

Liu, X., Zou, H., Slaughter, C., and Wang, X. (1997). DFF, a heterodimeric protein that functions downstream of caspase-3 to trigger DNA fragmentation during apoptosis. Cell *89*, 175–184.

Lu, Q., Zhang, X., Almaula, N., Mathews, C.K., and Inouye, M. (1995). The gene for nucleoside diphosphate kinase functions as a mutator gene in Escherichia coli. J. Mol. Biol. *254*, 337–341.

Ma, D., Xing, Z., Liu, B., Pedigo, N.G., Zimmer, S.G., Bai, Z., Postel, E.H., and Kaetzel, D.M. (2002). NM23-H1 and NM23-H2 repress transcriptional activities of nuclease-hypersensitive elements in the platelet-derived growth factor-A promoter. J. Biol. Chem. *277*, 1560–1567.

Monteiro, A.N. (2000). BRCA1: exploring the links to transcription. Trends Biochem. Sci. *25*, 469–474.

Nagata, K., Saito, S., Okuwaki, M., Kawase, H., Furuya, A., Kusano, A., Hanai, N., Okuda, A., and Kikuchi, A. (1998). Cellular localization and expression of template-activating factor I in different cell types. Exp. Cell Res. *240*, 274–281.

Nakajima, H., Park, H.L., and Henkart, P.A. (1995). Synergistic roles of granzymes A and B in mediating target cell death by rat basophilic leukemia mast cell tumors also expressing cytolysin/perforin. J. Exp. Med. *181*, 1037–1046.

Postel, E.H. (1999). Cleavage of DNA by human NM23-H2/nucleoside diphosphate kinase involves formation of a covalent protein-DNA complex. J. Biol. Chem. *274*, 22821–22829.

Postel, E.H., Berberich, S.J., Flint, S.J., and Ferrone, C.A. (1993). Human c-myc transcription factor PuF identified as nm23-H2 nucleoside diphosphate kinase, a candidate suppressor of tumor metastasis. Science *261*, 478–480.

Postel, E.H., Weiss, V.H., Beneken, J., and Kirtane, A. (1996). Mutational analysis of NM23–H2/NDP kinase identifies the structural domains critical to recognition of a c-myc regulatory element. Proc. Natl. Acad. Sci. USA *93*, 6892–6897.

Postel, E.H., Abramczyk, B.M., Levit, M.N., and Kyin, S. (2000). Catalysis of DNA cleavage and nucleoside triphosphate synthesis by NM23- H2/NDP kinase share an active site that implies a DNA repair function. Proc. Natl. Acad. Sci. USA *97*, 14194–14199.

Postel, E.H., Abramczyk, B.A., Gursky, S.K., and Xu, Y. (2002). Structure-based mutational and functional analysis identify human NM23-H2 as a multifunctional enzyme. Biochemistry *41*, 6330–6337.

Russell, J.H., and Ley, T.J. (2002). Lymphocyte-mediated cytotoxicity. Annu. Rev. Immunol. *20*, 323–370.

Sarin, A., Williams, M.S., Alexander-Miller, M.A., Berzofsky, J.A., Zacharchuk, C.M., and Henkart, P.A. (1997). Target cell lysis by CTL granule exocytosis is independent of ICE/Ced-3 family proteases. Immunity *6*, 209–215.

Seo, S., McNamara, P., Heo, S., Turner, A., Lane, W.S., and Chakravarti, D. (2001). Regulation of histone acetylation and transcription by INHAT, a human cellular complex containing the set oncoprotein. Cell *104*, 119–130.

Seo, S.B., Macfarlan, T., McNamara, P., Hong, R., Mukai, Y., Heo, S., and Chakravarti, D. (2002). Regulation of histone acetylation and transcription by nuclear protein pp32, a subunit of the INHAT complex. J. Biol. Chem. *277*, 14005–14010.

Sharif-Askari, E., Alam, A., Rheaume, E., Beresford, P.J., Scotto, C., Sharma, K., Lee, D., DeWolf, W.E., Nuttall, M.E., Lieberman, J., and Sekaly, R.P. (2001). Direct cleavage of the human DNA fragmentation factor-45 by granzyme B induces caspase-activated DNase release and DNA fragmentation. EMBO J. *20*, 3101–3113.

Shi, L., Kraut, R.P., Aebersold, R., and Greenberg, A.H. (1992). A natural killer cell granule protein that induces DNA fragmentation and apoptosis. J. Exp. Med. *175*, 553–566.

Shikama, N., Chan, H.M., Krstic-Demonacos, M., Smith, L., Lee, C.W., Cairns, W., and La Thangue, N.B. (2000). Functional interaction between nucleosome assembly proteins and p300/CREB-binding protein family coactivators. Mol. Cell. Biol. *20*, 8933–8943.

Shresta, S., Graubert, T.A., Thomas, D.A., Raptis, S.Z., and Ley, T.J. (1999). Granzyme A initiates an alternative pathway for granule-mediated apoptosis. Immunity *10*, 595–605.

Steeg, P.S., Bevilacqua, G., Kopper, L., Thorgeirsson, U.P., Talmadge, J.E., Liotta, L.A., and Sobel, M.E. (1988). Evidence for a novel gene associated with low tumor metastatic potential. J. Natl. Cancer Inst. *80*, 200–204.

Tell, G., Zecca, A., Pellizzari, L., Spessotto, P., Colombatti, A., Kelley, M.R., Damante, G., and Pucillo, C. (2000). An 'environment to nucleus' signaling system operates in B lymphocytes: redox status modulates BSAP/Pax-5 activation through Ref-1 nuclear translocation. Nucleic Acids Res. *28*, 1099–1105.

Thomas, D.A., Du, C., Xu, M., Wang, X., and Ley, T.J. (2000). DFF45/ICAD can be directly processed by granzyme B during the induction of apoptosis. Immunity *12*, 621–632.

Toh, S.Y., Wang, X., and Li, P. (1998). Identification of the nuclear factor HMG2 as an activator for DFF nuclease activity. Biochem. Biophys. Res. Commun. *250*, 598–601.

Weaver, V.M., Lach, B., Walker, P.R., and Sikorska, M. (1993). Role of proteolysis in apoptosis: involvement of serine proteases in internucleosomal DNA fragmentation in immature thymocytes. Biochem. Cell Biol. *71*, 488–500.

Xanthoudakis, S., Miao, G., Wang, F., Pan, Y.C., and Curran, T. (1992). Redox activation of Fos-Jun DNA binding activity is mediated by a DNA repair enzyme. EMBO J. *11*, 3323–3335.

Zhang, D., Beresford, P.J., Greenberg, A.H., and Lieberman, J. (2001a). Granzymes A and B directly cleave lamins and disrupt the nuclear lamina during granule-mediated cytolysis. Proc. Natl. Acad. Sci. USA *98*, 5746–5751.

Zhang, D., Pasternack, M.S., Beresford, P.J., Wagner, L., Greenberg, A.H., and Lieberman, J. (2001b). Induction of rapid histone degradation by the cytotoxic T lymphocyte protease granzyme A. J. Biol. Chem. *276*, 3683–3690.